Infiltration Study for Deep Foundations in Ephemeral Streams

Naresh C. Samtani, *President, NCS GeoResources, LLC, Tucson, USA; email:* naresh@ncsgeoresources.com

ABSTRACT: *The duration of a flood event in an ephemeral stream is finite, ranging from a few hours to a few days. However, for design of deep foundations, an assumption is typically made by geotechnical specialists that at the time of a flood event all stream bed geomaterials are saturated and fully-buoyant. This assumption leads to larger deep foundations because full-buoyancy can significantly reduce the geomaterial resistances to applied loads. Consequently, a large increase in foundation investigation and construction costs can occur. This paper presents a case study that included an evaluation of the infiltration of transient flood waters into unsaturated geomaterials within an ephemeral stream bed. Considerable cost reductions were realized as a result of this evaluation. The presented approach permits a rational geotechnical evaluation of deep foundations in ephemeral streams.*

KEYWORDS: Infiltration, Ephemeral, Bridge, Deep Foundation, Unsaturated, Pore Water Pressure, Flood, Scour

SITE LOCATION: **Geo-Database**

INTRODUCTION

Bridge designers generally prefer use of deep foundations when scour is expected to occur at bridge crossings over streams. The word "stream" in this paper is used to mean a body of water that flows across the natural (i.e., unlined) ground surface and is contained within a channel with lined or unlined banks. In this sense, "stream" covers the full range from small waterways such as washes and creeks to large waterways such as rivers. A perennial stream is one which flows throughout the year. In contrast, an ephemeral stream experiences flows during, and for a limited time after, rainfall and/or discharge from an upstream water retention facility.

In perennial streams, the stream bed is saturated and the pore water pressure (PWP) is positive. The PWP at a depth z below the stream bed can be computed as $(\gamma_w)(z+h)$, where γ_w is the unit weight of water and h is the height of water above the stream bed. The positive PWP profile is linear (hydrostatic) and this condition is herein referenced as "fully-buoyant" (FB).

In ephemeral streams, a FB condition occurs only under the regional groundwater level (GWL) which could be at considerable depth below the stream bed. Depending on the grain size distribution (GSD) of the geomaterials a complex regime of PWP can occur between the stream bed and the GWL that is generally idealized into two zones as follows:

- A capillary saturation zone can occur for a limited height immediately above the GWL where the soil is saturated, but the PWP is negative representing a suction condition. The profile of the negative PWP can be computed using $-(\gamma_w)(z_a)$, where z_a is the distance above the GWL. Thus, in the capillary saturation zone, the negative PWP profile has the same linear trend as for the positive PWP below the GWL.

- Above the capillary saturation zone is the capillary fringe zone which extends to the stream bed. In this fringe zone, unsaturated (i.e., partially saturated) conditions occur and the profile of negative PWP is nonlinear. The magnitudes of the nonlinear negative PWPs in this zone are a function of the type of geomaterial, the degree of saturation (or water content), and climate factors at the stream bed (e.g., evaporation).

As the wetting front due to infiltrating water advances into an ephemeral stream bed the PWP profile changes. During a flood event, positive PWP can occur for a limited time in localized areas above the GWL. Depending on the water retention

capability and hydraulic conductivity (HC) of the geomaterials, the magnitude of this positive PWP can be less than the hydrostatic pressure in a FB condition. This condition is referenced herein as "partially-buoyant" (PB).

The PWP, whether positive or negative, has considerable impact on the shear strength and volume change characteristics of geomaterials. For the case of positive PWP the concept of effective stress as postulated by Terzaghi (1943) can be used while for the case of negative PWP postulations that consider matric suction are used (e.g., Bishop, 1960; Fredlund et al., 2012). As the PWP become positive the effective stress reduces. Coarse-grained soils are typical in ephemeral streams. For such soils the total unit weight typically ranges from 17 to 21 kN/m^3. Given that γ_w=9.8 kN/m^3 the effective stresses can be about 40 to 55% of the total geostatic stresses for the FB condition. Geomaterial side resistance to applied loading on a deep foundation in coarse-grained soils is often expressed as a function of effective stresses using a nonlinear multiplier that varies with depth, e.g., the β-multiplier (AASHTO, 2012). In such cases, at the FB condition, the geomaterial side resistance for a deep foundation is reduced in proportion to the decrease in effective stresses. Therefore, to carry the same applied vertical load, a larger (e.g., bigger cross-section and/or longer) deep foundation is necessary to compensate for the loss of effective stress. Depending on the methods chosen for analysis of deep foundations, similar considerations can also apply for tip (bottom or base) and lateral resistances.

This paper presents a case study where infiltration analyses were performed to evaluate the transient PWP profile between the stream bed and the GWL in an ephemeral stream and how this information was used for design of deep foundations.

BACKGROUND AND IMPETUS FOR STUDY

The impetus of this study was the Magee Road widening project in Tucson, AZ, for the Pima County Department of Transportation (PCDOT). For this project, a new 86.2 m long 3-span bridge was designed in 2010-2011 to carry the widened Magee Road over the Cañada Del Oro (CDO) Wash which is an ephemeral stream. The new bridge was planned immediately adjacent to an existing 85.6 m long 3-span bridge. The stream bed geomaterials were predominantly sands with varying amounts of gravels. The depth to GWL within the CDO Wash was about 45 m that is typical in the Tucson region. The existing bridge was constructed in 1983-1984 at which time the scour depth was estimated to be 6.6 m. Drilled shaft foundations of 1.2 m diameter extending to a depth of 10 m below scour elevation were constructed. The new bridge configuration was virtually identical to the existing bridge which meant that the foundation loads were approximately the same. Using the latest Pima County guidelines, the scour depth was estimated to be 7.6 m. In addition, PCDOT project criteria required bridge design to be developed in accordance with Arizona DOT (ADOT) practice. In ADOT practice, a FB condition during flood is assumed in ephemeral streams. Such an approach is typical for many agencies. As per this approach, the length of the drilled shafts for the new bridge was found to be about 60% more than the length of the shafts for the existing bridge leading to a large increase in foundation investigation and construction costs. This increase in length was easily explained by (a) earlier observation that for FB conditions the effective stresses are reduced in comparison with the total geostatic stresses, and (b) the deeper scour depth for the new bridge.

The finding of large increase in costs related to the foundations of the new bridge and perceived design deficiency in the existing bridge concerned PCDOT. Therefore, PCDOT initiated a review of the performance of the existing bridge and other similar bridges in the Tucson area. The review found 6 other bridges like the existing Magee Road bridge that were constructed between 1982 and 1988. In a memorandum (PCDOT, 2011), the PCDOT bridge engineer indicated that based on documented regular bridge inspections "all of the bridges built during that period are performing well. Our inspection reports indicate that there is no apparent settlement, movement, rotation or displacement of those bridges or any components of those bridges. These observations and reports lead us to believe that the original design for the drilled shafts has performed as intended." Thus, the observed performance of 7 existing bridges over a period of more than 25 years appeared to indicate the assumption of a FB condition during a flood event, which can lead to an overly conservative design, may not be warranted.

To help reconcile the considerable discrepancy between the good observed performance and ADOT-based practice, a preliminary evaluation of the PWP development within the stream bed was performed using the theory for infiltration reported by Green-Ampt (1911) and Warrick et al. (1985). This evaluation indicated that (a) during a flood event positive, PWPs were experienced in the stream bed for a shallow depth only, and (b) these transient positive PWPs dissipated quickly within a matter of few hours or days after the flood. These observations were corroborated by detailed field measurements made during a groundwater recharge research program by United States Geological Survey (USGS) as part of which infiltration rates within local ephemeral streams were evaluated (Hoffman et al., 2002, 2007). Considering these findings, PCDOT desired a detailed evaluation of infiltration and development of PWPs using site-specific data rather than indiscriminately using the assumption of FB condition that leads to large increase in foundation costs.

The detailed evaluation of site-specific infiltration was performed using SEEP/W software for numerical transient saturated/unsaturated seepage analyses. The results of the numerical modeling showed that the patterns of development of PWPs during a flood event and dissipation of PWPs after the flood event compared very well with those observed from the field measurements by USGS (Hoffman et al., 2002, 2007). Given these studies and the documented good performance of existing bridges, PCDOT made the decision to use 1.2 m diameter drilled shafts for the new Magee Road bridge. Using the site-specific PWP profile from the infiltration study, it was determined the lengths of the drilled shafts were similar to those for the existing bridge. Thus, PCDOT realized significant cost reductions by performing site-specific analysis.

Realizing the value of site-specific infiltration studies, PCDOT developed a formal protocol for performing infiltration study for bridge foundations in ephemeral streams. Using this protocol two new 185 m long 6-span bridges carrying the northbound and southbound La Cholla Boulevard over the CDO Wash were evaluated in 2011-2012 and significant cost reductions were also realized. In 2015, the protocol was used again during the design of the new Sunset Road (SR) connection from Silverbell Road to Interstate 10 (I-10) Frontage Road which included a 220 m long 6-span bridge over the ephemeral Santa Cruz River (SCR). As with the previous projects, similar cost reductions were also achieved. This paper describes the site-specific infiltration study performed for the Sunset Road SCR (SR-SCR) bridge which opened to traffic on February 14, 2017.

PROJECT SETTING

Figure 1 shows the location of the SR-SCR bridge site (32°18'20.42"N, 111° 2'56.71"W). The SCR, with headwaters in southern Arizona and northern Mexico, flows northwesterly along the west side of City of Tucson and roughly parallels I-10 and Silverbell Road in the project area. At the time of the geotechnical investigations, the existing ground surface along the longitudinal center line of the bridge varied from elevation (El.) 670 m at the lowest point (i.e., thalweg) of the SCR channel to about El. 675 m at the banks where the bridge abutments are located. The average ground surface between the abutments was at about El. 672 m. Wetlands and mesoriparian habitats occur in the project area.
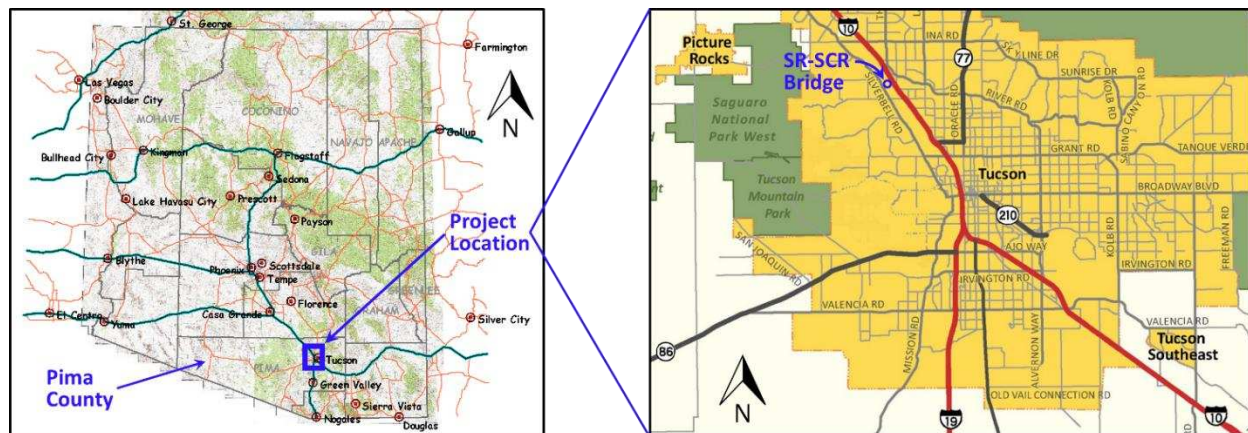

Figure 1. Project location and SR-SCR bridge site (base maps from PAG, 2019).

REGIONAL GEOLOGY

The project site is in the northwestern part of the Tucson Basin which is a broad 2,600 km^2 area in the upper SCR drainage basin located in Pima County, Arizona. The basin is filled with alluvial deposits eroded from the surrounding mountain ranges. At the project site, the estimated depth to bedrock is in excess of 525 m (AZGS, 2007). Three soil units are encountered at the project site. The near-surface soils include overbank deposits of silt, clay and fine sand, and channel deposits comprised of sand, gravel and cobbles transported from the surrounding mountains and alluvial terraces. These near-surface soils, which are collectively identified as Recent Alluvium ("Qal") unit by USGS (Davidson, 1973; Anderson, 1987), are randomly layered within the soil profile as a result of thousands of years of stream-channel meandering. Below the Qal unit lie older alluvial terrace deposits comprised of sand and gravel with varying amounts of clay. USGS (Davidson, 1973; Anderson, 1987) indicates these older units are part of the Fort Lowell Formation ("Qf") and Upper Tinaja bed ("Tsu"). TW (1987) data indicates that in the vicinity of the project site, the geological contact between the Qf and Tsu dips down slightly (about 1 degree) in the northeast direction.

GEOTECHNICAL INVESTIGATION PROGRAM

The geotechnical investigation program at the SR-SCR bridge site included intrusive investigations in the form of 7 borings to retrieve disturbed and undisturbed samples, in situ testing in the form of Standard Penetration Tests (SPTs), and laboratory testing. In addition, hydrogeologic information developed by USGS (Davidson, 1973; Anderson, 1987; Hoffman et al. 2002, 2007), Tucson Water (TW, 1987), and Arizona Department of Water Resources (ADWR, 2013) was reviewed. These agencies have been engaged in extensive hydrogeologic investigations related to management of groundwater resources in the Tucson Basin, including groundwater recharge programs, and their data served as valuable benchmarks for comparing the site-specific soil properties in this study. Following is a summary of the investigations:

- One boring was drilled at each of the five pier and two abutment locations. The borings were drilled using truck- and track-mounted CME 75 drill rigs with 108 mm inside diameter (I.D.) and 206.4 mm outside diameter (O.D.) hollow-stem augers. The depths of these borings ranged from 48.9 to 49.2 m below the existing ground surface.

- The SPTs were performed in accordance with ASTM D 1586 at 1.5 m vertical intervals in each boring. The tests were staggered in adjacent borings so that information can be maximized at virtually all elevations within the borings. Disturbed samples were collected from a 34.9 mm I.D., 50.8 mm O.D., and 457.2 mm long standard split spoon sampler that was driven with an automatic hammer during the SPTs.

- Relatively undisturbed ring samples were obtained by driving a 63.5 mm I.D., 76.2 mm O.D., and 457.2 mm long ring sampler at specific locations. This thick-walled ring sampler was driven using the same automatic hammer used for SPTs. Thin-walled Shelby tube samplers were not feasible in the coarse-grained formations with varying gravel content.

- Groundwater was encountered in all 7 borings. The shallowest GWL was at El. 637 m and the deepest GWL was at El. 631 m. The Tucson region relies entirely on pumped groundwater from the Tucson basin for water consumption. This reliance on aquifer water has lowered the GWL. As a frame of reference, in the vicinity of project area, the GWL was at about El. 670 m in 1940 and El. 658 in 1985 (Anderson 1987; TW, 1987).

- Specific gravity (G_s) of soil solids was tested in accordance with ASTM D 854.

- The GSD was tested in accordance with ASTM D 422 and ASTM C 136 for samples from various depths within the borings. To develop GSD over a full range of grain sizes, hydrometer tests were also performed in accordance with ASTM D 1140. Characteristic (i.e., effective) grain sizes such as D_{60}, D_{50}, D_{30}, and D_{10} were obtained from these tests.

- The soil plasticity characteristics (Liquid Limit, LL, and Plastic Limit, PL) were tested in accordance with ASTM D 4318 on representative samples taken from various depths within the borings.

- Soils were classified in accordance with the Unified Soil Classification System (USCS) in ASTM D 2487.

- The in situ gravimetric water contents (GWCs) were tested in accordance with ASTM D 2216 on ring samples taken from various depths within the borings.

- Soil-water characteristic curves (SWCCs) were obtained from tests performed on ring samples in accordance with Method C of ASTM D 6836 by using pressure chamber equipment. Desorption (drying) SWCCs were developed. The samples tested were selected from various depths between existing grade and GWL.

- Data for in situ dry density (γ_d) were obtained from ring samples as well as from SWCC and GWC tests.

- Saturated vertical permeability, k_{satv}, was tested in accordance with ASTM D 2434 on remolded samples from various soil layers. The average in situ dry density and in situ water contents from each of the soil layers were used as the molding dry density and water content. The laboratory tests were performed in 152.4 mm I.D. rigid wall permeameters.

INTERPRETED SUBSURFACE CONDITIONS

Table 1 provides the idealized 3-layer subsurface profile used for foundation design and includes corresponding USGS units, elevation ranges, relative density, and USCS designations for the predominant soils. Varying gravel content was encountered in all layers. Presence of cobbles and boulders was inferred from the refusal blow counts (i.e., blows greater than 50 for

standard split spoon sampler penetration less than 150 mm), drill chatter, and limited sample recovery. The elevation ranges of USGS units noted in TW (1987) from a hydrogeologic viewpoint for a ground water recharge feasibility assessment project are nearly identical to those noted in Table 1. TW (1987) indicates the thickness of Tsu layer is more than 335 m.

Table 1. Idealized subsurface profile.

Layer	USGS Unit	Elevation Range, m	Relative Density	Predominant Soil Types
0	Qal	Ground surface – 666.0	Loose to medium dense	SM, GM, SC, GC, CL
1	Qf	666.0 – 653.8	Medium dense to dense	SM, SC
2	Tsu	653.8 – 621.5 (bottom of boring)	Dense to very dense	SM, SC, with cobbles and boulders

ENGINEERING PROPERTIES FOR INFILTRATION ANALYSIS

The average values of soil properties related to infiltration analysis and evaluation are listed in Table 2. Table 3 provides the number of tests (i.e., data points) used to calculate the various average values in Table 2. Following are the pertinent observations related to the tests performed and developed soil properties:

- The properties of Layer 1 and Layer 2 are of primary importance because, as discussed later with respect to Figures 4 and 5, the scour elevation is within Layer 1 and the infiltration into Layers 1 and 2 is of primary interest.

- Figure 2 shows the SWCCs that were developed using measured data from laboratory tests with the van Genuchten (1980) model and correction factor recommended by Fredlund et al. (2012) to direct the SWCC to a soil suction of 10^6 kPa at zero water content. However, the portion of the SWCCs in the high-suction (or "tail") portion is not utilized for the current infiltration analysis because the difference between the scour elevation (discussed later) and the GWL elevation is such that the maximum value of soil suction is approximately 215 kPa. The laboratory tests to develop SWCCs were carried to a suction value of 1,000 kPa which provides measured data well beyond the range of interest.

- The residual volumetric water content (VWC) values were obtained from the fit of the van Genuchten (1980) model to data from laboratory tests for determination of SWCCs.

- Figure 3 shows the Relative Hydraulic Conductivity (RHC) functions, which are normalized to k_{satv}=1.00 m/day at zero suction (i.e., FB condition) and express the variation of HC as a function of soil suction. These functions were estimated using SWCCs shown on Figure 2 by using the built-in van Genuchten algorithm in SEEP/W (2014). The layer specific HC function is obtained from the corresponding RHC function on Figure 3 by multiplying the normalized values on the ordinate of the RHC function with the chosen value of k_{satv} for soil in that layer.

- The values of n (porosity), VWC, and S (degree of saturation) were computed using phase relationships. The computations were first performed for each sample where a pair of GWC and γ_d values were available and then the average values were obtained. As a comparison, TW (1987) notes average porosity values of 0.30 and 0.29 for Qf (Layer 1) and Tsu (Layer 2) units, respectively. Thus, the values reported in Table 2 from site-specific investigations are consistent with those reported in TW (1987).

- The laboratory k_{satv} values using remolded samples are likely not representative of in situ conditions because while the in situ density and water content can be approximated during the remolding process, the in situ fabric of soils cannot be replicated. However, the laboratory k_{satv} values do provide information on the relative HC of different layers. From this perspective, it is found that the HC of Layer 2 could be almost 6 times smaller than that of Layer 1. The k_{satv} value of Layer 0, while documented in Table 2, is not of much importance in this study since most of the infiltration will occur in Layer 1 and Layer 2 (see Figure 5 and associated discussion later).

- Considering data from pumping tests in wells and aquifer recharge tests, TW (1987) notes that after accounting for anisotropy, the "equivalent" k_{satv} values range from 0.06 to 2.83 m/day in the Qf unit (Layer 1) and 0.08-0.69 m/day in the Tsu unit (Layer 2). TW (1987) indicates anisotropy values in the range of 1:10 to 1:100 for Qf unit and approximately 1:40 for Tsu unit. The reported anisotropy and equivalent k_{satv} values are for a long reach of the SCR within the Tucson Basin and not specific to the SR-SCR bridge site. Nevertheless, these values offer a frame of reference for the current study. In particular, the upper part of the ranges provided by TW (1987) indicate that Layer 2 is less permeable than Layer 1, which is consistent with the laboratory k_{satv} values. The fact that the values in the upper part of the range are larger than the values from laboratory tests confirms the limitation of modified soil fabric in remolded specimens.

- Due to the limitations of laboratory k_{satv} values and their contrast with k_{satv} values noted by TW (1987), it was important to establish a suitable range of HC functions for the SR-SCR bridge site. Therefore, "correlated k_{satv}" values were developed using empirical correlations with characteristic grain sizes and porosity. Since grain size and porosity data were available from many subsurface elevations, an opportunity to develop site-specific k_{satv} values was available. However, it was recognized that many empirical correlations are available which can give significantly different values. Therefore, rather than rely on a specific correlation, 6 empirical correlations attributed to Hazen, Slichter, Terzaghi, Beyer, Sauerbrei, and USBR, as noted in Vuković and Soro (1992), were evaluated. At each elevation in the subsurface where GSD and porosity values were available, correlated k_{satv} values were first developed for each of the 6 methods. Then, at a given elevation, an average of the k_{satv} values from the 6 methods was computed. This average k_{satv} value was considered representative of the in situ k_{satv} value at that given elevation. Using elevations, these average values were segregated into three layers and 28, 17, and 33 values of k_{satv} were obtained for Layer 0, 1 and 2, respectively. An average of the k_{satv} values in each layer (see Table 2) was determined for purpose of infiltration analysis. These average correlated k_{satv} values are larger than the laboratory k_{satv} values and the values reported by TW (1987). But all three sources (laboratory, TW and correlated) indicate that Layer 2 (Tsu) is less permeable compared to Layer 1 (Qf).

- The discrepancies in k_{satv} values are not surprising since it is well known that k_{satv} values can vary over several orders of magnitude. These observations emphasize the need for the infiltration analyses to consider a range of k_{satv} values.

Table 2. Average properties of soils.

Soil Property	Layer		
	0	1	2
SWCC function	See curves on Figure 2		
Residual VWC (m^3/m^3)	0.114	0.127	0.123
RHC function	See curves on Figure 3		
Laboratory k_{satv} (m/day)	0.32	0.23	0.04
Correlated k_{satv} (m/day)	5.33	5.39	3.69
D_{60} (mm)	1.034	3.638	3.415
D_{50} (mm)	0.626	2.275	2.096
D_{30} (mm)	0.200	0.642	0.548
D_{10} (mm)	0.047	0.048	0.041
LL (%)	13.9	16.7	13.4
PL (%)	9.0	8.9	8.7
GWC (%)	3.9	6.8	8.1
G_s (dim)	2.70	2.70	2.70
γ_d (kN/m^3)	16.2	17.9	18.9
n (dim)	0.39	0.32	0.30
VWC (%)	6.2	12.5	15.3
S (%)	16.0	40.3	52.1

Table 3. Number of tests used to calculate average values.

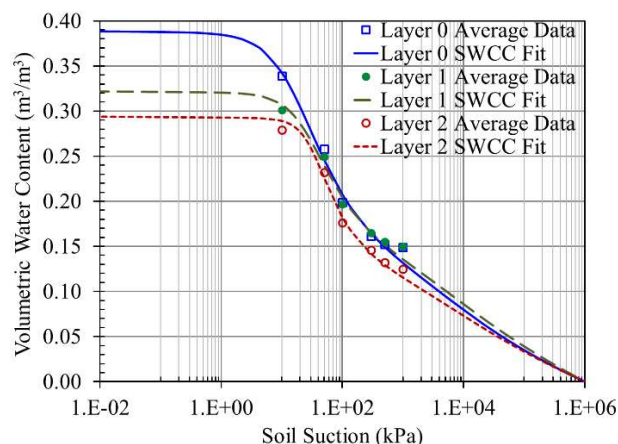| Soil Property	Layer		
	0	1	2
SWCC, Residual VWC, and RHC	2	4	7
Laboratory k_{satv}	2	1	2
Correlated k_{satv}	28	17	33
D_{60}, D_{50}, D_{30}, and D_{10}	28	17	33
LL and PL	28	17	33
GWC	6	16	31
G_s	2	4	7
γ_d	6	16	31
n, VWC, S (from phase relations)	6	16	31

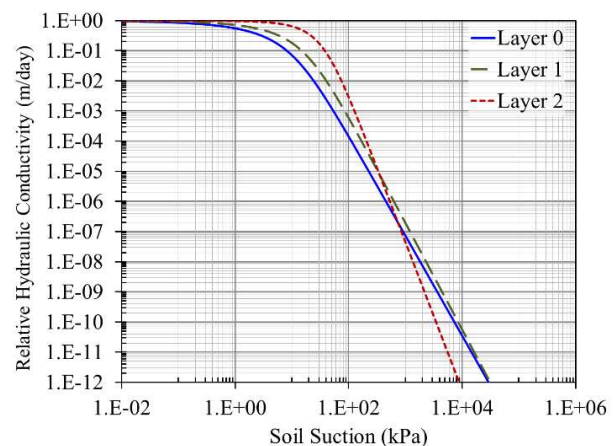*Figure. 2. Soil Water Characteristic Curves.*

Figure 3. Relative Hydraulic Conductivity Functions.

FLOOD CHARACTERISTICS

The two key flood hydraulic parameters for performing an infiltration analysis in ephemeral streams are the flood hydrograph and the scour elevation. Pima County Regional Flood Control District (PCRFCD, 2013) developed flood hydrographs for 100-year and 500-year events which have a 1% and 0.2% chance, respectively, of occurring every year. Both flood hydrographs consisted of 6 segments as shown on Figure 4, with the segment number encircled above the bottom x-axis. For each segment, these hydrographs express flood stage in terms of height and time in hours (or days). The total flood duration for both flood events is 96 hours (4 days). The maximum flood height, which occurs at 49 hours (2.04 days) for both events, is 7 m for the 500-year event and 6.25 m for the 100-year event. Table 4 provides the rate of hydraulic loading, r_{hl}, for each segment of both hydrographs.

In the development of the hydrographs, PCRFCD (2013) considered the largest recorded flood in the SCR that occurred in October 1983 (Roeske, et al. 1989) due to the tropical storm Octave. This flood caused significant damage to bridges and other properties within the flood plain including complete destruction of the old Sunset Road bridge, a Bailey type structure, located just downstream of the new SR-SCR bridge location. PCRFCD (2013) indicates that the following information was considered as part of its development of the hydrographs on Figure 4: (a) the October 1983 flood that peaked at 1,493 m^3/sec as measured at Congress Street stream flow gaging site which is about 12 km upstream of the SR-SCR bridge site, and (b) Pima County (1984) memorandum which specifies that designs for channels and bridges in the general project area of the SR-SCR bridge site be performed using a 100-year flood event with a peak discharge of 1,986 m^3/sec and a duration of 96-hours. Pima County (1984) had developed the 100-year flood event recommendation using a rainfall-runoff model that was calibrated using measurements from the October 1983 flood. The peak discharge value of 1,986 m^3/sec is 33% larger than measured value of 1,493 m^3/sec and PCRFCD (2013) indicates this was done to "provide additional conservatism for designing channels and bridges."
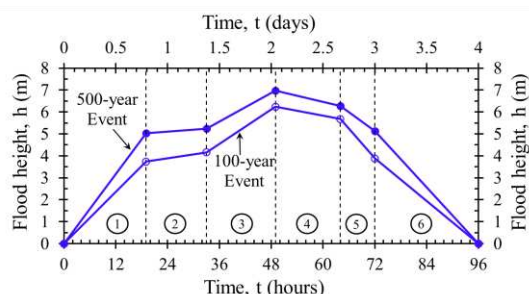

Figure 4. Flood hydrographs.

Table 4. Rate of hydraulic loading, r_{hl}.

Segment	Time Range		r_{hl} (m/day)	
	Hours	Days	500-year Event	100-year Event
1	0 - 19	0 - 0.79	+6.36	+4.72
2	19 - 33	0.79 - 1.38	+0.35	+0.73
3	33 - 49	1.38 - 2.04	+2.61	+3.11
4	49 - 64	2.04 - 2.67	-1.11	-0.89
5	64 - 72	2.67 - 3.00	-3.47	-5.38
6	72 - 96	3.00 - 4.00	-5.12	-3.88

Based on above considerations, PCRFCD (2013) developed the 100-year and 500-year event 96-hour duration hydrographs on Figure 4 that correspond to a discharge of 1,986 m^3/sec and 3,041 m^3/sec, respectively. As per PCRFCD (2013), the 500-year hydrograph represents a scaled-up version of the 100-year event and matches the discharge specified by FEMA (2012) in the project area as part of its flood insurance study. The discharge of 3,041 m^3/sec represents a 53% increase over the discharge of 1,986 m^3/sec which was already 33% more than the peak measured discharge during the October 1983 flood. This larger 500-year flood event results in overtopping of current channel banks. Given these considerations, PCRFCD (2013) indicates that the hydrographs provided on Figure 4 are "conservative."

SCOUR CHARACTERISTICS

Project hydraulic specialists from PCRFCD and the University of Arizona (UA, 2015) estimated total scour depths at piers and abutments for both flood events. The total scour depth is the summation of general/contraction scour, local scour, long-term bed degradation scour, and bend scour. The total scour elevations varied across the channel and were different for piers and abutments. For the 500-year event the total scour elevations ranged from 659 to 662.5 m. For the 100-year flood event, the total scour elevations ranged from 660.5 m to 665.3 m. After review of the total scour elevations, PCDOT directed that infiltration analysis and foundation design be developed using the conservative assumption of the lowest total scour elevation of 659 m and 660.5 m for 500-year and 100-year flood events, respectively. With respect to the average ground surface at El. 672 m, these scour elevations indicate scour depths of about 13 m and 11.5 m for the 500-year and 100-year flood events, respectively.

NUMERICAL MODEL FOR INFILTRATION ANALYSIS

The infiltration analysis was performed by using the finite element (FE) based SEEP/W (2014) software. This section discusses the analysis domain and initial conditions, boundary conditions, hydraulic properties, time-steps and convergence criteria used for the analysis. The 500-year flood event is used for discussions.

Analysis Domain and Initial Conditions

Figure 5 shows the two-dimensional (2-D) analysis domain. This figure defines several benchmark elevations as follows: HFL: Highest Flood Level; SL: Scour Level: BL1: Bottom of Layer 1; GWL: Ground Water Level; and BD: Bottom of Domain for analysis. The right boundary (Line F-G-H-I) and left boundary (Line A-M-L-K-J) were chosen to be sufficiently far away from the existing bank and scour scarp (Line B-C-D) such that flow patterns near the right boundary are not affected. The right boundary represents conditions towards the middle of the SCR channel. Thus, at the right boundary, the infiltrating water follows a vertical path towards the regional GWL (Line K-H) and maximum PWPs will occur. Hence, for deep foundation design the PWP profile at the right boundary is of primary interest. A fixed mesh was used. The mesh consists of first order 3-noded triangular and 4-noded quadrilateral elements with a total of 1,315 elements and 1,365 nodes. The approximate global element size was 1.524 m. As shown in Figure 6, smaller elements were used in the areas of high hydraulic gradients such as near the scour level, scour scarp, unlined bank, and layer boundaries. The initial conditions were expressed in terms of an idealized linear PWP profile with depth as shown on Figure 6.
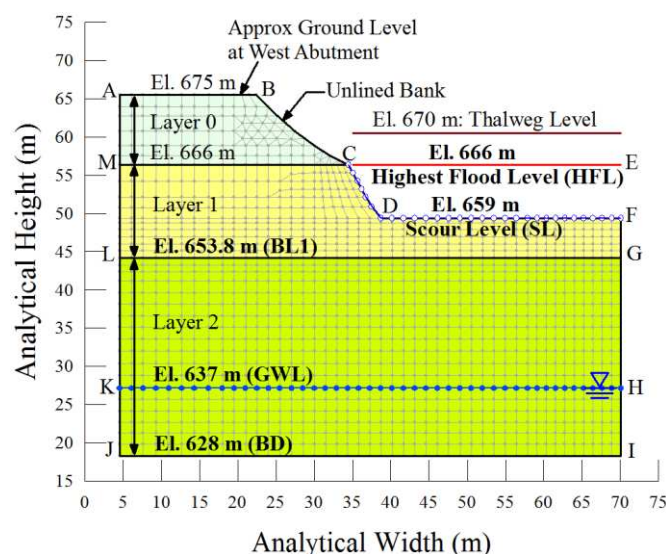

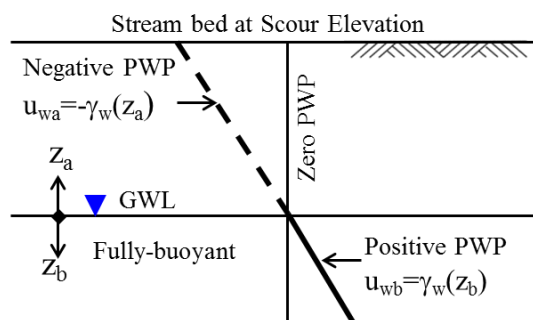*Figure 5. 2-D domain for infiltration analysis.*   *Figure 6. Initial conditions.*

Boundary Conditions

The 2-D model was formulated in terms of total head. The boundary conditions consisted of (a) the GWL (Line K-H) at El. 637 m (highest GWL measured in borings), and (b) the 500-year flood hydrograph on Figure 4 applied at the stream bed corresponding to the 500-year SL at El. 659 m (Line D-F). Since the maximum flood height for the 500-year event is 7 m, the HFL is at El. 666 m. The PWP is zero (i.e. total head equal to elevation) at the location of the GWL. Thus, the infiltration is caused by a difference in total head between the GWL and the 500-year hydrograph applied at SL. This difference is the flood height shown on Figure 4. Evaporation was not considered in the analyses because for deep foundation design the geotechnical resistances of interest occur well below the shallow depths where evaporation effects occur. Also, during a short and intense flood event represented on Figure 4, the evaporation effects are unlikely to affect the infiltration profiles.

Hydraulic Properties

Layers 0, 1, and 2 were assigned the SWCC and HC curves shown in Figures 2 and 3 respectively. The vertical and horizontal HCs were assumed to be equal in all layers, i.e., isotropic HCs were used. Since the goal of the study is to evaluate the effect

of flood-induced buoyancy on the geotechnical resistance of deep foundations, this assumption will lead to conservative results as more water will infiltrate downward leading to increased generation of the PWPs.

Time Steps and Convergence

The time steps chosen varied from 0.0002 days during a flood event up to 0.5 days after the flood event. This wide variation in time steps was required to capture the rapidly changing conditions at the beginning of a flood event without creating computational instabilities and to avoid unnecessary iterations at the end of a flood event and afterwards when minimal changes in pressure head and water content take place. An "adaptive" time-stepping technique included in the SEEP/W (2014) software was used. The adaptive time stepping routine inserts extra time steps between specified time steps in the event the solution is not meeting the specified time stepping or convergence criteria. The solution was considered converged if the difference in total head at a node was less than 0.03 m between successive iterations.

PARAMETRIC STUDY AND RESULTS

To account for inherent large uncertainty in HC, a parametric study was performed using the four cases in Table 5. Case 1 and Case 2 simulate the lower bound and upper bound of HC values, respectively. Case 3 evaluates the possibility Layer 2 may have smaller HC compared to Layer 1 due to which water can perch (pond or mound) in Layer 1 and create FB condition. Case 4 evaluates the possibility Layer 2 may have larger HC compared to Layer 1 due to which larger PWPs can develop in Layer 2.

Table 5. Summary of Cases for infiltration analyses.

Case	Characteristic	Isotropic k_{sat} (m/day)		
		Layer 0	Layer 1	Layer 2
1	HC using k_{satv} values from laboratory measurements	0.32	0.23	0.04
2	HC using k_{satv} values from correlations with GSD	5.33	5.39	3.69
3	HC using correlated k_{satv} for Layer 0 and 1; correlated $0.1k_{satv}$ value in Layer 2	5.33	5.39	0.37
4	HC using laboratory k_{satv} for Layer 0 and 1; correlated k_{satv} value in Layer 2	0.32	0.23	3.69

The PWP profiles for all four cases are illustrated on Figures 7 through 14 for the 500-year flood event. Results of analyses for the 100-year flood event were similar. The PWP profiles are shown in terms of head of water. The height of the flood, h, and r_{hl} at each time are noted in the caption of each figure. All the figures have the same format to allow for a direct comparison of results. In this context, the common reference features in the figures are as follows:

- Levels SL, BL1, GWL, and BD are as defined earlier on Figure 5. On Figures 7 through 10, FL denotes Flood Level at the time, t, noted in the figure captions.

- Line F-D-E, labelled IC, represents the initial condition, shown on Figure 6, that is also the lower bound for PWP

- Line B-C-G, labelled FB, represents the fully-buoyant condition where the PWPs are hydrostatic and upper bound.

- Line D-E represents the FB condition under the GWL. Note that the slope of Line D-E and Line B-C-H-G is the same.

- Line A-I-D-K represents zero PWP.

- The zone between Line A-I-D-K and Line F-D represents mainly unsaturated conditions wherein the PWPs are negative.

- In the zone between Line A-I-D-K and Line B-C-H, the PWPs are positive and represent a PB condition.

- Line A-B represents the hydrostatic pressure due to flood water. The PWP at stream bed level is represented by Line I-B. At the end (t=4 days) of the flood event and afterwards, the flood height, h is zero which leads to zero PWP at the stream bed level and Points A and B coincide with Point I (see Figures 11 through 14).

Following are observations related to PWP profiles on Figures 7 through 14:

- Between BL1 and GWL, the PWP profiles vary significantly in accordance with the k_{sat} value and the case in Table 5. In some cases, the PWP head becomes negative while in other cases the PWP head is positive, but in all cases the PWP head is less than hydrostatic as evidenced by the PWP profiles being to the left of Line C-H.

- Regardless of the case, all profiles merge at Point D which represents zero PWP at the GWL.

- Below the GWL, all PWP profiles coincide with Line D-E where FB condition occurs.

- Case 3 shows a PWP build-up that results in mobilization of FB condition in Layer 1 followed by a sharp drop-off in PWP in Layer 2. This shows the possibility of perched water as noted earlier.

Overall, the PWP profiles can be linear or nonlinear as seen on Figures 7 through 14. The PWP profiles vary depending on increasing flood height (Figures 7 through 9), decreasing flood height (Figures 10 and 11), and after the flood event (Figures 12 to 14). Following are some observations related to development and dissipation of PWP with time.

- t=0.6 days (Figure 7): For Cases 2 and 3, the slope of the PWP profile between SL and BL1 is to the right of Point B and towards Line BC. For Case 3, the FB condition is mobilized since k_{sat} value for Layer 2 is much smaller than Layer 1. In contrast, for Cases 1 and 4, the k_{sat} value of 0.23 m/day for Layer 1 is relatively small and mobilization of PWP is slow with the slope of the PWP profile between SL and BL1 to the left of Point B being towards Line F-D. The PWP profiles for Cases 1 and 4 overlap since the k_{sat} value of 0.23 m/day for Layer 1 is the same for both cases. In all cases $r_{hl} > k_{sat}$ and hence the flood waters that have not infiltrated into the stream bed advance downstream causing flow in the SCR.

- t=1 day (Figure 8): Although the rate of hydraulic loading has slowed, the flood height is larger. Thus, the previously infiltrated water is continuing to infiltrate further down as is reflected by the PWP profile for Cases 1 and 4 being deeper into Layer 1 compared to that on Figure 7. The PWP profiles for Cases 1 and 4 overlap since the k_{sat} value of 0.23 m/day for Layer 1 is the same for both cases.

- t=2 days (Figure 9): This time is close to 2.04 days when the maximum flood height occurs. The rate of hydraulic loading has also increased. It is observed that for Cases 1, 2, and 3, the PWP is positive in Layer 1 while for Case 4 the PWP becomes negative close to BL1. However, the patterns of positive PWP are different. For Case 3, a FB condition is achieved in Layer 1. For Case 2, the PWP profile shows a slight deviation to the right of Point B. For Cases 1 and 4, the PWP profiles show deviation to the left of Point B. In Cases 1, 3 and 4, the PWPs sharply reduce and become negative within approximately 5 m below BL1 and merge with the IC line. For Case 2, the PWPs reduce almost linearly to Point D. The PWP profiles for Cases 1 and 4 no longer overlap since the wetting front has migrated into Layer 2 and the k_{sat} values for Layer 2 are different for these two cases (see Table 5).
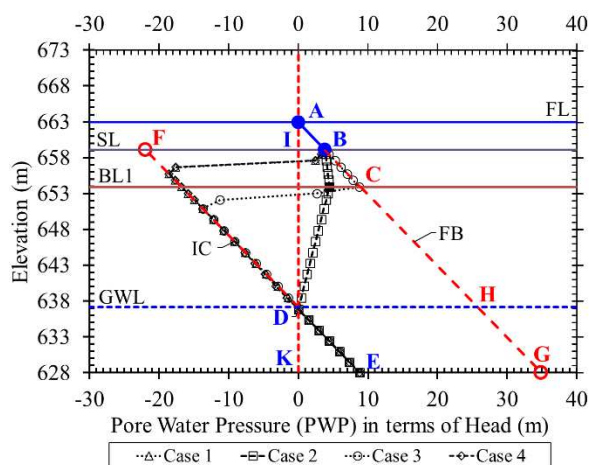

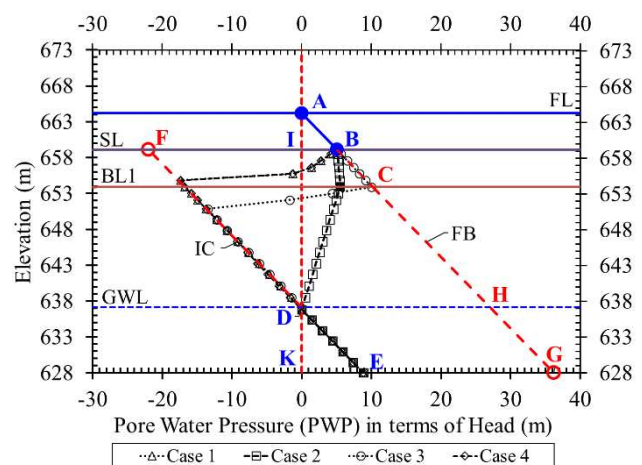*Figure 7. PWP at t=0.6 days (h=3.82 m, r_{hl}=+6.36 m/day).*   *Figure 8. PWP at t=1 day (h=5.11 m, r_{hl}=+0.35 m/day).*
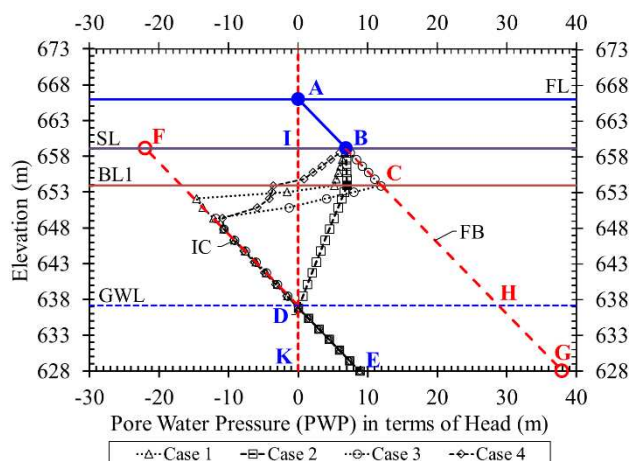
Figure 9. PWP at t=2 days (h=6.87 m, r_{hl}=+2.64 m/day).

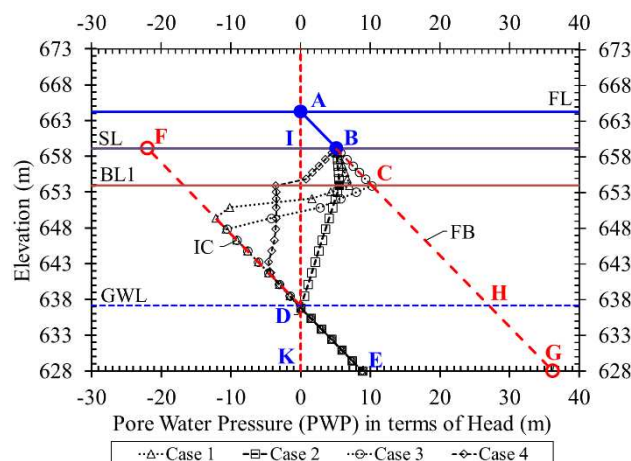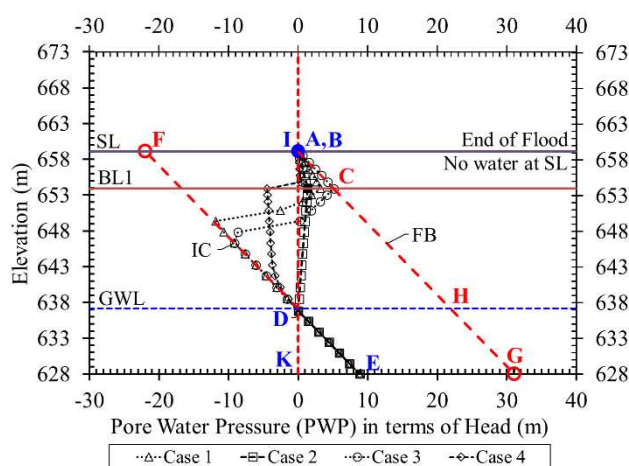*Figure 10. PWP at t=3 days (h=5.12 m, r_{hl}=-1.15 m/day).*

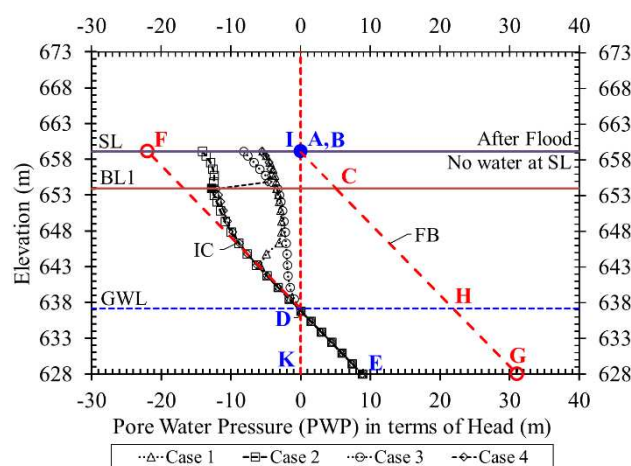*Figure 11. PWP at t=4 days (h=0 m, r_{hl}=0 m/day).*

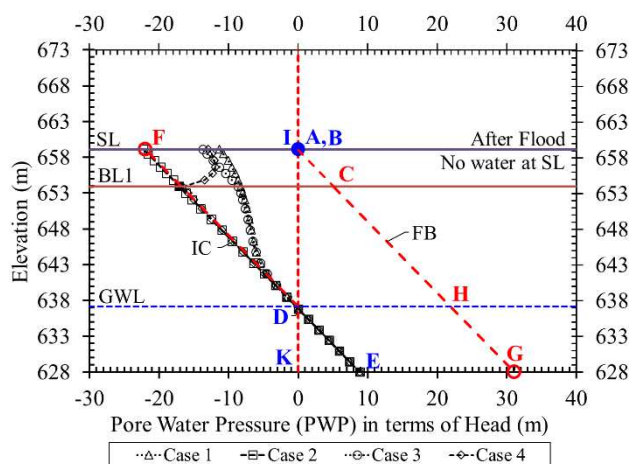

Figure 12. PWP at t=30 days (h=0 m, r_{hl}=0 m/day).

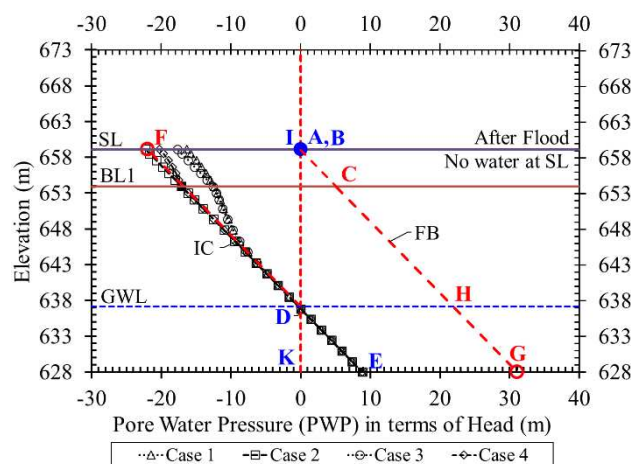
Figure 13. PWP at t=384 days (h=0 m, r_{hl}=0 m/day).

Figure 14. PWP at t=1824 days (h=0 m, r_{hl}=0 m/day).

- t=3 days (Figure 10): At this time, even though the flood is receding, the flood height is still significant and coupled with the previously infiltrated water, the wetting front continues to proceed further towards the GWL. The PWP profiles for all four cases are now distinctly different with Case 2 showing an almost linear PWP profile in Layer 2 compared to the nonlinear PWP profiles for other cases in Layer 2. While the flood height is approximately the same at t=1 day (h=5.11 m) and t=3 days (h=5.12 m), the PWP profiles shown on Figures 8 and 10 are different because the r_{hl} values are different.

- t=4 days (Figure 11): At this time, the flood has ceased. Except for Case 3 PWP profile between SL and BL1 being at FB condition, the PWP profiles in all instances (including for Case 3 below BL1) recede towards Line F-D-E. The pattern and rate of recession is different depending on the case considered. This is to be expected because the infiltration process is directly affected by the k_{sat} values and the HC functions.

- t=30 days (Figure 12): At this time, about 1 month has elapsed since the start of the flood. All the cases show negative PWP profiles above the GWL and to the left of Line I-D-K.

- t=384 days (Figure 13) and t=1824 days (Figure 14): These times correspond to 1.05 years and 5 years after start of flood. The PWP profiles continue to recede further towards Line F-D-E. Before reaching Line F-D-E, the PWP profiles are nonlinear above the GWL. All PWP profiles merge into the linear trend below Point D which is to be expected.

PWP PROFILE FOR DEEP FOUNDATION DESIGN

Many combinations of parameters listed in Table 2 and flood events are possible. Furthermore, many other factors can affect the PWPs. For example, the flood hydrographs could be different than those shown on Figure 4, the soils may have localized variations within a given layer, SWCC hysteresis could be possible, air pressure (u_a) in pores may have an effect, the concentration of suspended solids (i.e., turbidity) in flood waters may retard infiltration, scour surface may vary across the channel, etc. For deep foundation designs the PWP head profile that gives the largest positive PWP is of interest since it will lead to the largest reduction in effective stress. Accordingly, the maximum PWP at all computation depths for each of the cases in Table 5 was extracted from the results and plotted as shown on Figure 15. The PWPs for each of the four cases shown on Figure 15 do not occur at the same time but they represent a profile of maximum value of PWP. Thus, the PWP profiles are conservative. The conservatism is further increased because the effect of matric suction due to negative PWPs as reflected in increased shear resistance is disregarded by considering only the maximum PWPs that are greater than or equal to zero. Based on an evaluation of the maximum PWP profiles, a PWP envelope (Line B-C-D-E) below SL was developed for design of the deep foundations for the SR-SCR bridge. The PWP envelope covers for the possibility of different combinations of parameters and other factors as discussed above. In the PWP envelope, the PWP is hydrostatic between SL and BL1 (segment B-C). Between BL1 and GWL, the PWP head profile is assumed to vary linearly (segment C-D). Below GWL, the PWP is represented by a hydrostatic condition (segment D-E). In segments B-C and D-E a FB condition occurs. In segment C-D, PB condition occurs.
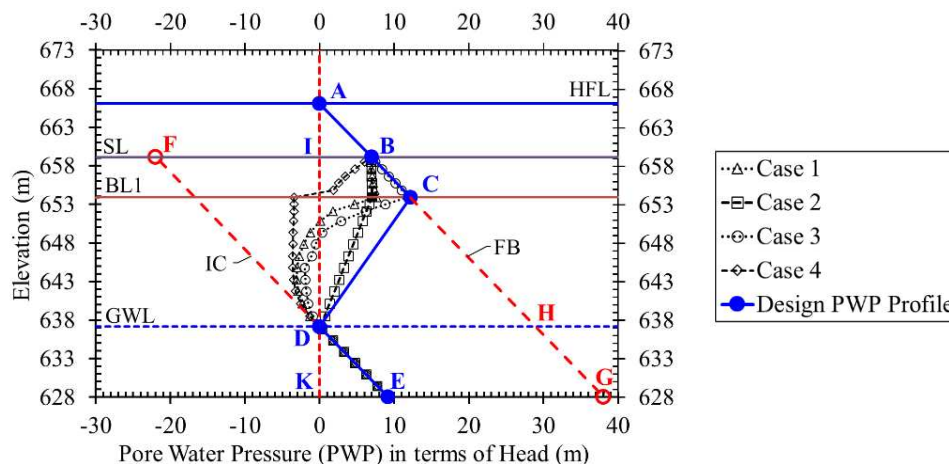

Figure 15. Maximum PWP profiles and PWP envelope for 500-year flood event at the SR-SCR bridge site.

PWP CRITERIA AND OTHER ASSUMPTIONS FOR DEEP FOUNDATION DESIGN

Several PWP profiles as shown on Figure 16 were developed for deep foundation design in terms of various elevations (HFL, SL, BL1, GWL, and BD) noted on Figure 5. The values of these elevations for the 100-year and 500-year flood events have been defined earlier. On Figure 16, the following conditions are represented:

- FB condition: Line A-B-C-H-G

- No-buoyancy (NB) condition: Line I-J-D

- PB condition: Between Line B-C-H and Line I-J-D

- PWP Envelope (PE) condition: Line A-B-C-D-E

- Rapid drawdown (RD) condition: Line I-C-D-E

The rapid drawdown (RD) condition accounts for the scenario that the flood recedes quickly after reaching HFL but the flood water is trapped (ponds) above BL1 as was observed for Case 2. This condition is more critical than the PE condition because the effective stress between SL and BL1 for RD condition will be lesser than in the PE condition.
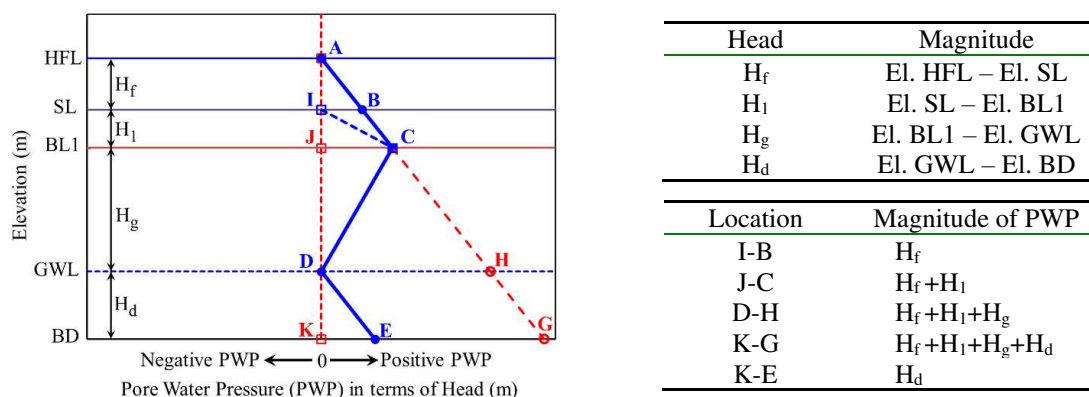

Head	Magnitude
H_f	El. HFL – El. SL
H_1	El. SL – El. BL1
H_g	El. BL1 – El. GWL
H_d	El. GWL – El. BD

Location	Magnitude of PWP
I-B	H_f
J-C	$H_f + H_1$
D-H	$H_f + H_1 + H_g$
K-G	$H_f + H_1 + H_g + H_d$
K-E	H_d

Figure 16. Design PWP profiles for a flood event at the SR-SCR bridge site.

It is prudent to be conservative when designing bridges where floods and scour are a consideration. In this regard, the notable design assumptions to develop conservative deep foundation design for the SR-SCR bridge are as follows: (1) the channel is suddenly and uniformly scoured to a level surface, (2) the lowest possible total scour level is used, (3) the entire flood hydrograph is applied at the deepest level scoured surface, (4) the hydrograph of the flood event is developed conservatively, (5) subsurface anisotropy is disregarded which in turn leads to faster vertical infiltration and mobilization of PWPs, (6) the regional dip of the Qf/Tsu geological contact which would promote lateral flow above the contact surface and reduce infiltration into the Tsu layer is disregarded, (7) the flood waters are clear (i.e., no turbidity) and will penetrate into a clean level interface between the water and stream bed, (8) pore air pressures that can inhibit water movement and reduce the rate of infiltration rate and build-up of PWP are not considered, (9) an envelope to the maximum positive PWP profiles is used in which negative PWPs that develop matric suction are disregarded, (10) rapid drawdown scenario is evaluated, and (11) side and lateral resistance above the idealized level total scour surface is neglected. Any of these assumptions by itself leads to some level of conservatism in foundation design. For example, rather than a level scour surface, during a flood event the scour depth will be relatively deeper at the foundation location due to local scour and shallower elsewhere and in such a configuration infiltration rates and PWP generation will be smaller as the infiltrating water has to navigate its way through this uneven scour surface. Taken together all the assumptions provide a compounded level of conservatism in foundation design. Thus, even though the PWP profiles on Figure 16 appear to be much smaller than the FB condition, conservatism will still exist in the foundation design process.

With respect to the PWP profiles it is important to realize that while the SCR channel at the bridge site is about 200 m wide the underlying aquifer is several kilometers wide. The porosity value of Layers 1 and 2 is approximately 30% (see Table 2) and this fact coupled with the deep GWL means the stream bed has a very large storage capacity. Due to this condition, the entire flood represented by the hydrograph on Figure 4 will be easily absorbed and dispersed over the large Tucson Basin

aquifer and the stream bed will continue to be in the unsaturated regime. Thus, development of a FB condition is not possible at the SR-SCR bridge site.

DEEP FOUNDATION DESIGN

Deep foundations for bridges typically consist of driven piles or drilled shafts. Due to the dense to very dense soils and the presence of cobbles and boulders, driven piles were not considered feasible. This is because in such conditions it would make it difficult to drive the piles to required depths without damaging them. Therefore, drilled shaft foundations were utilized. Use of drilled shafts also helped mitigate noise issues that could potentially affect wetlands and mesoriparian habitats in the project area.

The analysis and design of drilled shafts was performed in accordance with the Load and Resistance Factor Design (LRFD) Bridge Design Specifications of AASHTO (2012). The equations for estimating nominal unit side resistance, q_{SN}, and nominal unit tip (bottom or base) resistance, q_{BN}, for cohesionless soils are based on use of a depth-dependent side load-transfer coefficient, β, and N_{60} values, respectively. The N_{60} value is the hammer efficiency corrected SPT N-value given as $N_{60}=1.33N$. The value of q_{SN} is obtained from $q_{SN}=\beta\sigma'_v$ where β is expressed as $\beta=X(1.5-0.245z^{0.5})$, z is the depth in meters, $X=1$ for $N_{60}\geq15$, $X=N_{60}/15$ for $N_{60}<15$, $0.25<\beta<1.2$ and σ'_v is the effective vertical stress at depth z that is obtained by subtracting the positive PWP from the total overburden stress σ_v. The PWP≥0 corresponding to a given head, H, is obtained from Figure 16 as the $(\gamma_w)(H)$ for the case analyzed, i.e., the PE or RD case. The value of q_{BN} is expressed as $q_{BN}=58N_{60}$ for $N_{60}\leq50$ and the limiting q_{BN} value is 2.9 MPa. Thus, in the AASHTO (2012) formulation, the effective stress influences the side resistance directly while the tip resistance is a function of N_{60} value.

As per the LRFD approach, Strength, Service, and Extreme Event limit states were analyzed. The Strength and Service limit state evaluations were performed using the 100-year flood event while the Extreme Event limit state evaluation was performed using the 500-year flood event. At each support location, a single row of 3 drilled shafts was used (Figure 17). Table 6 provides a summary of the shaft diameter, D, total length L_T, top and tip elevations, and embedded length, L_E, below the 100-year SL at El. 660.50 m. The drilled shaft design was performed by considering resistances only in the embedded portion below SL. The drilled shaft dimensions in Table 6 were developed for the RD condition which was found to govern the design as discussed below.
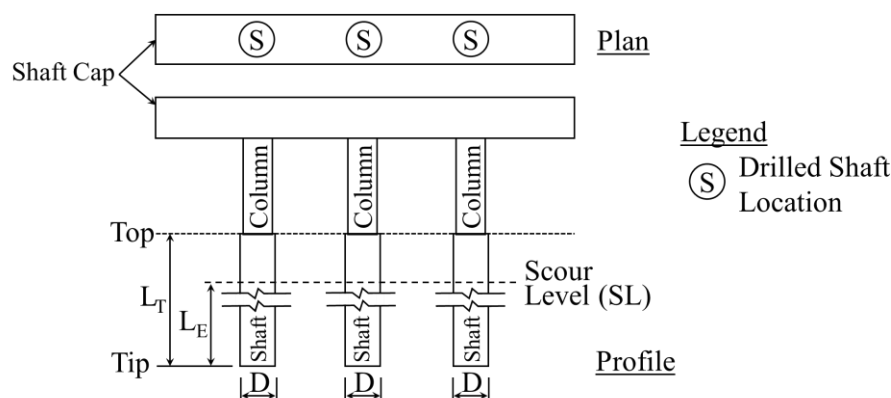

Figure 17. Schematic of drilled shaft configuration and dimensions at a given support.

Table 6. Drilled shaft dimensions.

| Support (Label) | D, m | L_T, m | Elevations, m | | L_E, m |
			Top	Tip	
Abutment 1 (A1)	2.44	35.58	673.23	637.65	22.85
Pier 1 (P1), Pier 2 (P2)	1.83	42.83	672.85	630.02	30.48
Pier 3 (P3)	1.83	40.46	670.48	630.02	30.48
Pier 4 (P4)	1.83	42.14	672.16	630.02	30.48
Pier 5 (P5)	1.83	43.66	673.68	630.02	30.48
Abutment 2 (A2)	2.44	41.99	675.67	633.68	26.82

All tip elevations in Table 6 are below BL1 at El. 653.8 m. Thus, all drilled shafts were embedded deep into Layer 2. To evaluate the effect of site-specific infiltration analysis on deep foundation design, a comparison of the FB, NB, PE and RD conditions is included in Tables 7 through 9. The comparison is based on tip elevation in Table 7, L_T in Table 8, and L_E in Table 9. The values of L_T in Table 8 were computed by subtracting the tip elevations in Table 7 from the top elevations noted in Table 6. As with Table 6, L_E is the embedded length below the 100-year SL at El. 660.50 m. The difference in shaft length (L_T or L_E) between PE and RD conditions is +1.21 m (5.6%) at support A1, +2.44 m (8.7%) at support P1 to P5, and +2.13 m (8.6%) at support A2. Thus, for the RD condition longer shafts are needed. Therefore, the RD condition was considered the governing condition and was adopted for drilled shaft design noted in Table 6.

Table 10 provides the comparison of NB, PE and RD conditions with respect to the FB condition. The comparison is provided in terms of change in embedded length (ΔL_E) and the corresponding percent. The ΔL_E values were obtained by subtracting the L_E for the FB condition from L_E for other conditions in Table 9. The % change for NB condition varies from 40.5 to 44.4%. As expected, for the PE and RD conditions the % change values reduce, but the change is still substantial between 30.1 and 38.6%. Clearly, even after consideration of conservative PWP profile, and other conservative assumptions noted earlier, the reductions in shaft lengths for the PE and RD conditions are significant.

Table 7. Comparison of tip elevations.

Support	Condition and Tip El., m			
	FB	NB	PE	RD
A1	625.45	641.00	637.65	638.86
P1, P2	616.92	634.59	630.02	632.46
P3	616.92	634.59	630.02	632.46
P4	616.92	634.59	630.02	632.46
P5	616.92	634.59	630.02	632.46
A2	620.27	637.34	633.68	635.81

Table 8. Comparison of L_T.

Support	Condition and Total Length, L_T, m			
	FB	NB	PE	RD
A1	47.78	32.23	34.37	35.58
P1, P2	55.93	38.26	40.39	42.83
P3	53.56	35.89	38.02	40.46
P4	55.24	37.57	39.70	42.14
P5	56.76	39.09	41.22	43.66
A2	55.40	38.33	39.86	41.99

Table 9. Comparison of L_E.

Support	Condition and Embedded Length, L_E, m			
	FB	NB	PE	RD
A1	35.05	19.50	21.64	22.85
P1, P2	43.58	25.91	28.04	30.48
P3	43.58	25.91	28.04	30.48
P4	43.58	25.91	28.04	30.48
P5	43.58	25.91	28.04	30.48
A2	40.23	23.16	24.69	26.82

Table 10. Change in L_E compared to FB condition.

Support	ΔL_E, m (% change)		
	NB condition	PE condition	RD condition
A1	-15.55 (44.4%)	-13.41 (38.3%)	-12.20 (34.8%)
P1, P2	-17.67 (40.5%)	-15.54 (35.7%)	-13.10 (30.1%)
P3	-17.67 (40.5%)	-15.54 (35.7%)	-13.10 (30.1%)
P4	-17.67 (40.5%)	-15.54 (35.7%)	-13.10 (30.1%)
P5	-17.67 (40.5%)	-15.54 (35.7%)	-13.10 (30.1%)
A2	-17.07 (42.4%)	-15.54 (38.6%)	-13.41 (33.3%)

COST REDUCTIONS

For the dimensions noted in Table 6, the PCDOT project team estimated drilled shaft construction cost of $2.59 million using unit costs of $3,936/m and $2,624/m for 2.44 m and 1.83 m diameter shafts, respectively. The unit costs were based on (a) history of bid prices for similar shafts on recent projects in Tucson region and (b) use of slurry (i.e., "wet") method of shaft construction which the drilled shaft contractor utilized during the construction phase.

Without the infiltration analysis, the shaft lengths would have been those noted in the column for FB condition in Table 8. By using the infiltration analysis, the shaft lengths can be reduced as noted in the column for RD condition in Table 8. The cost reduction should not be estimated by linearly scaling the unit costs based on shaft lengths for the FB and RD conditions. In this case, the additional shaft length based on FB condition is not only deeper into the ground but also positions the shaft tips below the GWL which significantly increases the level of difficulty and level of risk in maintaining stable drill holes for the duration of construction. Thus, estimating the complete cost reduction entails consideration of many factors including, but not limited to: more time for drilling a given shaft, larger equipment capable of drilling deeper shafts and lifting larger and/or longer reinforcing cages which also requires more splicing; more concrete and reinforcing steel; increased potential for drill hole instability; more slurry in the case of "wet" drilling; more integrity and other construction testing; and more

labor effort. These considerations can cause the FB unit costs to increase in the range of 20 to 30%. Using an average increase in unit costs of 25%, the cost reduction was estimated to be about $1.67 million.

In addition to the above discussed costs, the costs related to geotechnical investigations during design phase would also increase because each of the drilled borings needs to extend a minimum of 3 shaft diameters or 6 m, whichever is larger, below the anticipated tip elevation of the deep foundations. This is a common stipulation (e.g., AASHTO, 2012) to ensure subsurface exploration extends to an adequate depth below the anticipated tip elevation to identify adverse soft conditions that can create a punching shear type of bearing failure. Given the shaft lengths for FB condition in Table 8, the borings would need to be extended to depths of up to about 62 m which is considerably more than the depths of about 49 m that were explored. Finally, from the owner's construction perspective, for longer shafts, more labor effort is needed for construction inspection and management personnel as well as additional data processing. The cost reduction related to these aspects were estimated to be about $0.1 million. Thus, overall, $1.77 million in cost reduction was estimated to have been realized by utilizing a site-specific infiltration analysis.

SUMMARY, GENERAL GUIDANCE, AND CLOSURE

A site-specific analysis to evaluate the infiltration of transient flood into unsaturated geomaterials of an ephemeral stream bed has been presented. The presented approach uses accepted principles of unsaturated soil mechanics and stream hydraulic engineering as part of which site-specific soil properties, flood hydrograph, and scour depths are rationally integrated to develop more realistic PWP profiles for deep foundation design.

To realize cost reductions for deep foundations, vertical and/or lateral load tests are performed to obtain better site-specific resistance values rather than use lower-bound resistance prescribed by national codes such as AASHTO. The approach presented in this paper is like the concept of a load test in that it can be considered a numerical hydraulic load test wherein the hydraulic loads, as represented by the flood event and scour depth, are used to generate site-specific PWP profiles rather than using larger PWPs based on the FB condition. Considerable cost reductions can be realized even if deep foundation design uses conservative PWP profiles and design parameters based on site-specific infiltration analysis rather than assuming FB stream bed during flood events.

It is critical to ensure that the Quality Control (QC) and Quality Assurance (QA) processes during construction are appropriately tailored to ensure the validity of design assumptions. For drilled shafts this includes requiring stringent inspection of shaft construction and evaluation of integrity tests with test tubes located on the outside perimeter of a reinforcing cage to evaluate any anomalies that might affect the structural integrity of the shafts. Such evaluations of shaft structural integrity should be performed by qualified and trained personnel who have been closely involved in the drilled shaft design process and not any third party that may not have an appropriate knowledge of the project and design assumptions.

Infiltration analysis may not be universally applicable at all locations within ephemeral streams. In some locations, fine-grained layers that can perch water may occur at various depths. Such situations were encountered at other bridge locations along SCR and other streams in the Tucson region. In other situations, the GWL may be at shallow depth below the stream bed level in which case the stream may be classified as an intermittent stream instead of ephemeral stream. In such situations, FB conditions may be more appropriate for foundation design. Thus, application of the approach demonstrated in this paper must be (a) carefully evaluated in the context of local hydrogeology and stream characteristics, and (b) always performed on a site-specific basis by qualified specialists. As part of this effort, the project owners must also identify potential future land use in the vicinity of the bridge site and establish appropriate design criteria. For example, sand and gravel pit mining operations are common in ephemeral stream beds (as was the case with the SR-SCR bridge site) and the location of the pits in vicinity of a given bridge site may affect flood and scour characteristics.

Infiltration studies require close interaction between specialists from various disciplines such as flood plain, hydraulic, hydrogeologic, geotechnical, and structural in coordination with project managers and owners. As can be surmised from this paper, there are many intricacies to be considered in infiltration analysis. Every bridge project should be considered critical when it involves flood and scour events. Thus, it is crucial to develop appropriate site-specific data (e.g., soil properties, flood hydrograph, scour elevation, etc.) and infiltration analysis and not indiscriminately apply results from one project to another, nor attempt to extrapolate results from one project to another, due to the appearance of them being similar.

About one third of the land surface of the world is arid or semi-arid, an environment in which ephemeral streams occur. In the USA the arid and semi-arid southwestern part is among the fastest growing regions. There are over 616,000 bridges in the USA (NBI, 2019) and hundreds of bridge crossings in arid and semi-arid regions (e.g., California, Arizona, Nevada, New Mexico, etc.). Use of the infiltration analysis approach demonstrated in this paper can help realize more rational and economical bridge foundation designs in ephemeral streams.

ACKNOWLEDGEMENTS

REFERENCES

American Association of State Highway and Transportation Officials (AASHTO), (2012). *AASHTO LRFD Bridge Design Specifications, 6th Edition.*

Arizona Department of Water Resources (ADWR), (2013). *Groundwater Site Inventory*. <https://gisweb.azwater.gov/waterresourcedata/>.

Anderson, S. R. (1987). "Cenozoic Stratigraphy and Geologic History of the Tucson Basin, Pima County, Arizona." *United States Geological Survey*. Water-Resources Investigations Report 87-4190, prepared in cooperation with the City of Tucson, 23.

American Society for Testing and Materials (ASTM), (2014). *Annual Book of ASTM Standards, Section 4, Volume 4.08, Soil and Rock (I): D420-D5876 and Volume 4.09, Soil and Rock (II): D5876-Latest*.

Arizona Geologic Survey (AZGS), (2007). *Estimated Depth to Bedrock in Arizona. Digital Geologic Map Series DGM-52, 2007, Version 1.0, Authors: Richard, S. M., Shipman, T. C., Greene, L. C., and Harris, R. C*.

Bishop, A.W. (1960). "The Principle of Effective Stress." *Norwegian Geotechnical Institute*, 32, 1-5.

Davidson, E. S. (1973). "Geohydrology and Water Resources of the Tucson Basin, Arizona." *United States Geological Survey*, Water-Supply Paper 1939-E, United States Geological Survey, prepared in cooperation with the City of Tucson, the U.S. Bureau of Reclamation, and the University of Arizona, 81.

Federal Emergency Management Agency (FEMA), (2012). *Flood Insurance Study, Volume 1 of 5, For Pima County, Arizona and Incorporated Areas, Federal Emergency Management Agency, Flood Insurance Study Number 04019CV001B*.

Fredlund, D. G., Rahardjo, H. and Fredlund, M. D. (2012). *Unsaturated Soil Mechanics in Engineering Practice*, John Wiley & Sons, New York, NY.

Green, W. H., and Ampt, G. A. (1911). ''Studies on Soil Physics: 1. Flow of Air and Water Through Soils.'' *The Journal of Agricultural Science*, 4(1), 1–24.

Hoffmann, J.P., Ripich, M.A. and Ellett, K.M., (2002). "Characteristics of Shallow Deposits Beneath Rillito Creek, Pima County, Arizona." *United States Geological Survey*, Water-Resources Investigations Report 01-4257, prepared in cooperation with the Arizona Department of Water Resources, , Tucson, AZ.

Hoffmann, J.P., Blasch, K.W., Pool, D.R., Bailey, M.A. and Callegary, J.B. (2007). "Estimated Infiltration, Percolation, and Recharge Rates at the Rillito Creek Focused Recharge Investigation Site, Pima County, Arizona," *USGS Professional Paper 1703-H, Ground-Water Recharge in the Arid and Semiarid Southwestern United States-Chapter H,* United States Geological Survey, Denver, CO, 185-220.

NBI (2019). "National Bridge Inventory." <https://www.fhwa.dot.gov/bridge/nbi.cfm>.

PAG (2019). "Pima Association of Governments". <http://webcms.pima.gov/cms/one.aspx?portalId=169&pageId=34155> (May 26, 2019).

Pima County Department of Transportation (PCDOT), (2011). "Performance of Existing County Bridges Supported by Drilled Shaft Foundations." *Memorandum from Dave M. Zaleski, Bridge Engineer, to Rick Ellis, Engineering Division Manager.*

Pima County Regional Flood Control District (PCRFCD), (2013). "Hydrograph for Geotechnical Evaluation – Santa Cruz River at Sunset Road." *Memorandum from Evan Canfield, Civil Engineering Manager, to Bill Zimmerman, Deputy Director.*

Pima County (1984). "Santa Cruz River Revised Discharges." *Memorandum from Charles Huckelberry, Director of Pima County Transportation and Flood Control District, to All Engineers.*

Roeske, R.H., Garrett, J. M., and Eychaner, J. H. (1989). "Floods of October 1983 in Southeastern Arizona." *United States Geological Survey.* Water-Resources Investigations Report 85-4225-C, prepared in cooperation with the U.S. Army Corps of Engineers, U.S. Bureau of Reclamation, and Arizona Department of Water Resources, Tucson, AZ.

SEEP/W (2014). "Groundwater Seepage Analysis with SEEP/W – An Engineering Methodology." *GeoStudio 2012 December 2014 Release, Version 8.14.1.10087, GEO-SLOPE International Ltd., Calgary, Alberta, Canada.*

Terzaghi, K. (1943). *Theoretical Soil Mechanics*, John Wiley and Sons, New York, NY.

TW (1987). "Tucson Recharge Feasibility Assessment." *Final Draft Phase A, Task 5, Hydrogeologic Evaluations for Recharge Sites, Prepared for Tucson Water by CH2M Hill in association with Errol L. Montgomery & Associates, Inc. and L. G. Wilson.*

UA (2015). *Bridge Scour Report for the Proposed Sunset Bridge.* Submitted to Pima County Department of Transportation by the University of Arizona.

Van Genuchten, M. Th. (1980). "A Closed-Form Equation for Predicting the Hydraulic Conductivity of Unsaturated Soils," *Journal of the Soil Science Society of America*, 44, 892-898.

Vuković, M. and Soro, A. (1992). *Determination of Hydraulic Conductivity of Porous Media from Grain-Size Composition.* Water Resources Publications, Littleton, CO.

Warrick, A. W., Lomen, D. O, and Yates, S. R. (1985). "A generalized solution to infiltration." *Soil Sci. Soc. Am. J.,* 49, 34-38.

NOTATIONS

2-D	Two-dimensional
A1	Abutment 1
A2	Abutment 2
AASHTO	American Association of State Highway and Transportation Officials
ADOT	Arizona Department of Transportation
ADWR	Arizona Department of Water Resources
ASTM	American Society for Testing and Materials
AZ	Arizona
AZGS	Arizona Geological Survey
BD	Bottom of Domain for analysis
BL1	Bottom of Layer 1
CDO	Cañada Del Oro
CME	Central Mine Equipment
D	Diameter of drilled shaft
D_{10}	Characteristic (i.e., effective) grain size for which 10% of weight is finer
D_{30}	Characteristic (i.e., effective) grain size for which 30% of weight is finer
D_{50}	Characteristic (i.e., effective) grain size for which 50% of weight is finer
D_{60}	Characteristic (i.e., effective) grain size for which 60% of weight is finer
DOT	Department of Transportation
El.	Elevation
FB	Fully-buoyant
FE	Finite Element
FL	Flood Level
G_s	Specific Gravity
GSD	Grain Size Distribution

GWC	Gravimetric Water Content
GWL	Regional Ground Water Level
h	Height of water above stream bed (also height of flood or flood height)
H_1	Head of water based on difference between El. SL and BL1
H_d	Head of water based on difference between El. GWL and BD
H_f	Head of water based on difference between El. HFL and SL
H_g	Head of water based on difference between El. BL1 and GWL
HC	Hydraulic Conductivity
HFL	Highest Flood Level
IC	Initial Condition
I.D.	Internal Diameter
kN	Kilonewton
km	Kilometer
kPa	Kilopascals
k_{sat}	Isotropic saturated permeability
k_{satv}	Saturated vertical permeability
L_E	Embedded length of drilled shaft
LL	Liquid Limit
LRFD	Load and Resistance Factor Design
L_T	Total length of drilled shaft
m	Meter
m^3	Cubic meter
mm	Millimeter
n	Porosity
N-value	Blow counts based on Standard Penetration Test (SPT)
N_{60}	Hammer efficiency corrected SPT N-value
NB	No-buoyancy
NBI	National Bridge Inventory
O.D.	Outside Diameter
P1	Pier 1
P2	Pier 2
P3	Pier 3
P4	Pier 4
P5	Pier 5
PB	Partially-buoyant
PCDOT	Pima County Department of Transportation
PCRFCD	Pima County Regional Flood Control District
PE	PWP Envelope
PL	Plastic Limit
PWP	Pore Water Pressure
q_{BN}	Nominal unit tip resistance
q_{SN}	Nominal unit side resistance
Qal	Recent Alluvium
QA	Quality Assurance
Qf	Fort Lowell Formation
QC	Quality Control
r_{hl}	Rate of hydraulic loading
RD	Rapid Drawdown condition
RHC	Relative Hydraulic Conductivity
S	Degree of Saturation

SCR	Santa Cruz River
sec	Second (in time)
SEEP/W	A software for numerical transient saturated/unsaturated seepage analyses
SL	Scour Level
SPT	Standard Penetration Test
SR	Sunset Road
SR-SCR	Sunset Road bridge over the Santa Cruz River
SWCC	Soil-water Characteristic Curve
t	Time
Tsu	Upper Tinaja bed
TW	Tucson Water
UA	University of Arizona
USA	United States of America
USBR	United States Bureau of Reclamation
USCS	Unified Soil Classification System
USGS	United States Geological Survey
VWC	Volumetric Water Content
X	A ratio of N_{60} value to a specific N_{60}-value
z	Depth below stream bed
z_a	Distance above the regional ground water level (GWL)
β	Side load transfer coefficient
γ_d	In situ dry density
γ_w	Unit weight of water
ΔL_E	Change in embedded length
σ_v	Total overburden stress
σ'_v	Effective overburden stress
$	United State Dollar (currency)
%	Percent

INTERNATIONAL JOURNAL OF
GEOENGINEERING
CASE HISTORIES